33rd Annual International Conference of the IEEE EMBS
Boston, Massachusetts USA, August 30 - September 3, 2011

A Fully Automatic Method to Register the Prostate Gland on T2-weighted and EPI-DWI images

Massimo De Luca, Valentina Giannini, Anna Vignati, Simone Mazzetti, Christian Bracco, Michele Stasi, Enrico Armando, Filippo Russo, Enrico Bollito, Francesco Porpiglia, Daniele Regge

Abstract— **Prostate adenocarcinoma (PCa) is the most frequent noncutaneous cancer among men in developed countries. Magnetic Resonance (MR) has been used to detect PCa and several clinical trials report on the accuracy of the test. Multiparametric MR imaging (mpMRI) is defined as the integration of information from different morphological and functional datasets. mpMRI could be used to increase the performances of prostate MR, therefore allowing a more accurate assessment of the tumor gland extent, while reducing reporting time and interobserver variability. The first step to perform such a multiparametric analysis is to correct for voluntary and involuntary movements during the acquisitions, as well as for image distortion in the Diffusion Weighted (DWI) images. The aim of this work is to present a fully automatic registration algorithm between T2w and DWI images, able to realign the images and to correct the distortions in the DWI. Results showed a good overlap after registration and a strong decrease of mean surface distance in both the central gland and peripheral zone. These promising results suggest that the algorithm could be integrated in a CAD system which will combine the pharmacokinetic parameters derived from DCE-MRI, T2w MRI and DWI MR to generate one comprehensive value assessing the risk of malignancy. However to perform such a multiparametric analysis, it is necessary to correct for voluntary and involuntary (breathing, heart beating) movements during the DCE-MRI acquisition, and to realign also the DCE-MRI sequence to the T2w sequence.**

I. INTRODUCTION

Prostate adenocarcinoma (PCa) is the most frequent noncutaneous cancer among men in developed countries. The 2007 report from the American Cancer Society projected 218,890 new cases of prostate cancer and 27,050 additional deaths due to the disease in the United States [1] and its incidence is increasing because of the aging population. Since the advent of the prostate-specific antigen (PSA) era, wider screening has led to an increasing proportion of men with an elevated PSA but a negative digital rectal examination (DRE) [2]. Transrectal ultrasound (TRUS)-guided core prostate biopsies are being used routinely to systematically sample the entire gland in patients with abnormal DRE and/or elevated PSA in the search for prostate cancer and the histopathologic examination of biopsy tissue remains the gold standard for diagnosing prostate cancer. However, the sensitivity and specificity of TRUS in diagnosing impalpable prostate cancer still remains low: the number of false negatives in a single sextant biopsy session reported ranges between 30 and 45% [3]. Limitations of traditional screening methods are stimulating research in the field of diagnostic imaging, because accurate tumor detection, localization, and staging may critically influence the choice of treatment, radical (prostatectomy, hormone ablation, radiotherapy) versus local, minimally invasive therapies (cryoablation, radiofrequency ablation, focused ultrasound) that can improve quality of life without compromising oncologic outcome. Some patients with low-risk prostate cancer may also be candidates for the watchful waiting approach. While diagnostic T2-weighted (T2w) MRI images are a sensitive noninvasive imaging technique for detecting focal abnormalities in the prostate, they lack specificity distinguishing between tumor and benign prostatic hyperplasia (BPH) and other abnormalities. In fact, it is reported that T2w MR has a specificity of 43%, and a sensitivity of 85% for nonpalpable, posteriorly located tumors [4]. Thus, there is a need to improve the image-based specificity to diagnose cancer and to integrate information from other MR methodologies or imaging modalities. An alternative to T2w MRI is to develop image contrast through "apparent diffusivity" (tissue water incoherent displacement over distances of 1–20 mm). Diffusion-weighted (DWI) magnetic resonance imaging has been used in both clinical and research settings for detecting cerebral pathologies [5]. Recently, reports of the utility of DWI in prostate cancer [6], [7] have been presented. The extensive branching ductal structure of the normal prostate compared with the highly restricted intracellular and interstitial spaces encountered in prostate cancers produces a substantial differential in apparent diffusion coefficient (ADC), and thus the potential for high image contrast. DWI MR has extreme sensitivity to motion and, consequently, requires ultrafast imaging techniques. With the recent advances in MR hardware development, particularly fast gradient coils, single-shot echo planar imaging (EPI) emerged as a technique of choice for diffusion measurements in intra-abdominal organs as well as the prostate gland. With EPI sequence an image is acquired within a single shot, the duration of which is typically around 100 msec, and hence motion is effectively frozen during the acquisition. EPI, how-

This work was supported by FPRC – Fondazione Piemontese per la Ricerca sul Cancro, Candiolo, Turin, Italy

Massimo De Luca, Anna Vignati, Enrico Armando, Filippo Russo, Daniele Regge are with Institute for Cancer Research and Treatment, Radiology Unit, Candiolo, Turin, Italy.

Valentina Giannini is with Politecnico of Turin, Electronics Department, Turin, Italy and with Institute for Cancer Research and Treatment, Radiology Unit, Candiolo, Turin, Italy. valentina.giannini@polito.it

Simone Mazzetti, Christian Bracco, Michele Stasi are with Institute for Cancer Research and Treatment, Medical Physics, Candiolo, Turin, Italy.

Enrico Bollito is with San Luigi Gonzaga Hospital, Anatomical Pathology Department, Orbassano, Turin, Italy.

Francesco Porpiglia is with San Luigi Gonzaga Hospital, Oncologic Urology Department, Orbassano, Turin, Italy.

ever, is affected by geometric distortions and chemical shift artifacts caused by the susceptibility effects. These effects are due to the air-filled balloon surrounding the endorectal coil and poor local B0 homogeneity which leads to pixel shifts, particularly in the phase encode direction. Jezzard [8] proposed a method to correct geometric distortion which requires the measure of the magnetic field map inside the FOV with the object to scan in place. Such a field map will include the effects of inhomogeneities of the main magnetic field and varying tissue susceptibility, then values from the field map can then be compared with the expected values and the distortion calculated and corrected. This method achieved good performance but is difficult to implement in normal clinical practice. Other methods are semi automatic and require the manual placement of control points on both T2w and DWI images [6], [7]. The aim of this work is to present a new fully automatic method to register T2w and EPI-DWI images which does not require the estimation of the static magnetic field and which is based on the automatic segmentation of the bladder and the endorectal coil. Bladder and endorectal coil are well-defined structures in both T2 and DWI and are easy to segment, while automatic prostate segmentation is challenging due to the heterogeneity of this anatomical region. This registration algorithm could be integrated in a computer aided diagnosis (CAD) system which will combine the pharmacokinetic parameters derived from DCE-MRI with information coming from T2w MRI and DWI MR to generate one comprehensive value assessing the risk of malignancy. This multiparametric analysis has recently been proven to be useful [9], but its performance strictly relies on an accurate registration between DWI MR and other MR modalities.

II. MATERIALS AND METHODS

A. MRI Protocols

DWI MR data were acquired on 12 patients using a single-shot EPI sequence with the following parameters: FOV=16 cm, slice thickness 3 mm, BW=62.50 kHz, TR=6275 ms, TE=min, flip angle=90, 128x128 matrix, b-value=600 s/mm^2, NEX=6, 24 slices. Apparent diffusion coefficient (ADC) values were calculated from two DWI images acquired with b-value=0 s/mm^2 and 600 s/mm^2. The ADC maps were reconstructed by calculating the ADC values in each pixel of each slice.

B. Database Development

In order to validate the proposed registration method, the peripheral zone (PZ), the central gland (CG) and the whole prostate gland (TOT) were manually drawn by a radiologist on both DWI and T2w images. In Fig. 6 are shown, both superimposed on the T2w image, the outlines of PZ and CG binary masks drawn on DWI (red line) and the outlines of the same regions drawn on the T2w (green) before (Fig. 6a) and after (Fig. 6b) the application of the registration method. Two performance indexes were calculated before and after registration: the overlap index (OI), defined as the ratio between intersection and union of the masks, and the mean surface distance (MSD). A total of 12 patients were included in this study, 4 exams were used as training set in order to find the optimal decreasing displacement rate (k in (1)) maximizing the overlap index, then the algorithm was validated on the remaining 8 exams. A t-test is performed to evaluate the p values between OI and MSD values before and after registration. The null hypothesis is that there is no difference between OI and MSD values before and after registration, with a significance level of 0.05.

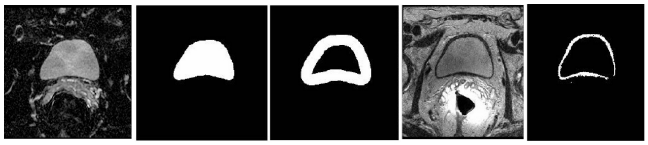

Fig. 1: *a) Bladder on DWI image. b) Segmented bladder on DWI. c) Stripe around bladder wall on DWI d) Bladder on T2w image. e) Segmented bladder wall on T2w image.*

C. Methods

The entire registration procedure involves two major steps. First, an affine transform is estimated by a segmentation-based method. In this step the bladder is automatically segmented in the DWI image by a watershed algorithm applied on the apparent diffusion coefficient (ADC) map, where it is well visible because of its high water content. The watershed is computed over the gradient magnitude image and proceeds in several steps. First, an initial classification of all points into catchment basin regions is done by tracing each point down its path of steepest descent to a local minima. Next, neighboring regions and the boundaries between them are analyzed according to a saliency measure, which is, in this case, the minimum boundary height, to produce a tree of merges among adjacent regions. Then, excluding the background, the bladder is the biggest region obtained with an absolute minimum height percentage of 10% and a depth of the catchment basin of 30%. As the bladder segmentation on DWI is obtained, morphological erosion and dilation are applied to extract a stripe around the border of the bladder (Fig. 1c). The stripe thickness is 20 mm, so it always includes the bladder wall also on the T2w image. Pixels belonging to this stripe on the T2w image were classified by a k-means cluster in two groups according to their intensity values, and the segmentation of the bladder wall is obtained, as is shown in Fig. 1e.

Then bladder border points on the T2w and DWI are extracted from the binary masks (Fig. 2) and coupled using the iterative closed points (ICP) algorithm (Fig. 3) in the slice where the bladder reaches its biggest area. The coupled points are used to find, by a least squares fitting, the affine transform parameters and then the transformation is applied on the whole DWI image.

The affine transform computed in the previous step can correct possible shearing, translational and scaling artifacts mainly caused by motion or by eddy currents (residual

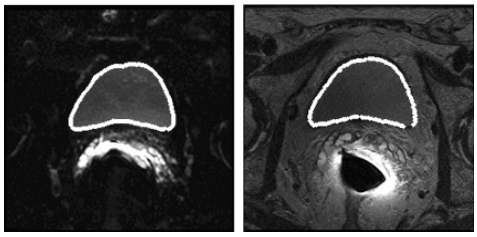

(a) (b)

Fig. 2: *Segmented bladder on the DWI image (a) and T2 image (b).*

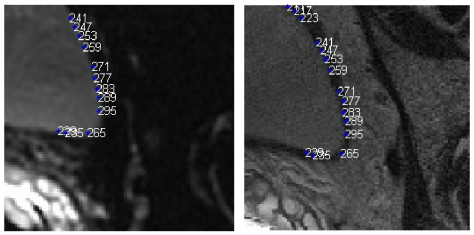

(a) (b)

Fig. 3: *Some of the bladder border points matched with ICP on DWI (a) and T2W (b) images.*

gradient field) formed in presence of a changing magnetic field [10], but do not correct non-linear geometric distortion caused in large part by static magnetic field inhomogeneities near the coil, and which is a major concern because most prostate tumors are localized in the peripheral zone. Therefore the first rigid registration step is refined with a non-rigid registration step based on the coil segmentation. The coil is segmented both in T2w and DWI images by a region growing algorithm, starting from a seed point inside the coil which is automatically found by a circular Hough transform. Then, for each slice where the coil is visible, two spline smoothing curves are fitted on the coil border points on the DWI and T2w images and used to estimate the displacement near the coil surface (Fig. 4). The initial displacement is estimated as the difference between the upper points of these spline curves, as shown in Fig. 4. Therefore the deformation field T is modeled as a piecewise linear decay field along the vertical direction (Eq. 1), assuming that the pixel shifts caused by magnetic field inhomogeneities occur particularly in the phase encode direction [8] and decrease linearly with distance from the coil.

$$T(x) = 0$$
$$T(y) = \begin{cases} d_i - k * y & 0 < y < \frac{d_i}{k} \\ 0 & y > \frac{d_i}{k} \end{cases} \quad (1)$$

where the coordinate system is shown in Fig. 4. The decreasing rate of the vertical displacement k in (1) was chosen maximizing the overlap index described in the following section on a training set. Then the estimated deformation

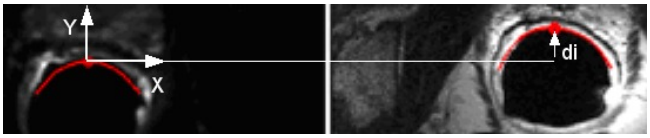

Fig. 4: *Spline curves superimposed on DWI (left) and T2w (right), and initial displacement between DWI and T2w near the coil.*

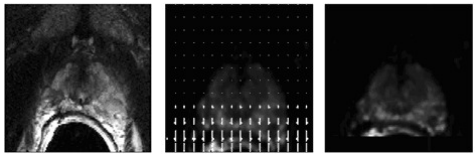

(a) (b) (c)

Fig. 5: *a) Prostate on T2 image. b) Deformation field superimposed on DWI. c) Deformation field applied on DWI.*

field T is applied to the DWI in order to correct the geometric distortion (Fig. 5).

III. RESULTS

Table I reports the MSD values and Table II the OI values for CG, PZ and TOT before and after registration. P-values for MSD measurements for CG, PZ and TOT are respectively 0.017, 0.0018 and 0.0014, while p-values of OI measurements are 0.015, 0.0004 and 0.0001 respectively. All p-values are smaller than the significance level, showing that the OI and the MSD obtained before registration are statistically different from those obtained after registration.

IV. DISCUSSION

In this study we presented an automatic registration algorithm able to correct misalignment between T2w and DWI MR images, due to a) incorrect determination of the resonance frequency by the scanner in some measurements leading to a "rigid body" shift in the phase-encoding direction of the echo planar images, b) susceptibility inhomogeneities resulting in irregular distortions, e.g. proximal to rectal wall at the air-tissue interface, and c) voluntary and involuntary patients movements during the acquisition. To the best of our knowledge there are no methods in literature addressing this problem in an fully automatic way. De Souza et al. [6] corrected the displacement by shifting the DWI images according to the amount of displaced center of mass, manually calculated. Automatic methods have the potential of reducing inter- and intra-observer variability and reading time, and could be integrated in a fully automatic CAD system for prostate cancer detection and diagnosis. One limitation of this method is represented by the choice of the parameters for the piecewise linear decay modeling. These parameters are heuristic constants chosen in order to obtain the best

TABLE I: *MSD for CG, PZ, TOT zones pre- and post- registration. Δ represents the % difference between the MSD pre and post registration.*

	CG pre mm	PZ pre mm	TOT pre mm	CG post mm	PZ post mm	TOT post mm	Δ CG	Δ PZ	Δ TOT
Patient 1	0.54	2.40	0.50	0.13	1.10	0.14	-76%	-54%	-72%
Patient 2	0.46	3.90	0.58	0.12	1.38	0.15	-74%	-65%	-74%
Patient 3	0.64	1.54	0.66	0.23	0.29	0.13	-64%	-81%	-80%
Patient 4	0.34	1.85	0.59	0.25	0.71	0.26	-26%	-62%	-56%
Patient 5	1.36	0.16	1.33	0.25	0.12	0.12	-82%	-25%	-91%
Patient 6	0.63	0.91	0.29	0.76	0.46	0.15	21%	-49%	-48%
Patient 7	0.30	2.45	0.65	0.13	0.20	0.11	-57%	-92%	-83%
Patient 8	0.47	1.50	0.55	0.18	0.45	0.10	-62%	-70%	-82%
Mean	0.59	1.84	0.64	0.26	0.59	0.15	-52%	-62%	-73%
Std. dev.	0.33	1.12	0.30	0.21	0.44	0.05	34%	20%	14%

TABLE II: *OI for CG, PZ, TOT zones pre- and post- registration. Δ represents the % difference between the OI pre and post registration.*

	CG pre	PZ pre	TOT pre	CG post	PZ post	TOT post	Δ CG	Δ PZ	Δ TOT
Patient 1	0.70	0.27	0.73	0.84	0.51	0.85	20%	89%	16%
Patient 2	0.70	0.28	0.70	0.84	0.53	0.83	20%	89%	19%
Patient 3	0.59	0.36	0.66	0.75	0.68	0.83	27%	89%	26%
Patient 4	0.73	0.32	0.65	0.71	0.58	0.71	-3%	81%	9%
Patient 5	0.41	0.21	0.51	0.79	0.69	0.84	93%	229%	65%
Patient 6	0.72	0.53	0.79	0.72	0.57	0.84	0%	8%	6%
Patient 7	0.74	0.32	0.71	0.79	0.73	0.85	7%	128%	20%
Patient 8	0.70	0.46	0.71	0.80	0.63	0.86	14%	37%	21%
Mean	0.66	0.34	0.68	0.78	0.62	0.83	22%	94%	23%
Std. dev.	0.11	0.10	0.08	0.05	0.08	0.05	30%	66%	18%

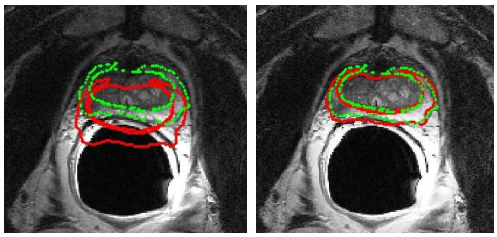

(a) (b)

Fig. 6: *Manual prostate gland segmentation drawn on DWI(red) and T2 (green) superimposed on T2, before registration (a) and after registration(b)*

performance on the training set. Future works should include the choice of such parameters based on a optimization step, i.e. including mutual information, in order to obtain more reproducible results and better generalize the problem. In conclusion, we presented a method to automatically register images coming from two different datasets (T2w and DWI), and results showed a good overlap after registration and a strong decrease of mean surface distance in both the central gland and peripheral zone, 0.26 mm and 0.59 mm respectively. Other studies in literature obtained a mean distance of 1.2 mm [6] in a semi-automatic way, or 0.5 mm [8], by calculating the RMS field inhomogeneity variations. The algorithm should be certainly tested on a larger dataset, but its promising results suggest that it could be integrated in a CAD system which will combine the pharmacokinetic parameters derived from DCE-MRI, T2w MRI and DWI MR.

REFERENCES

[1] A. Wolf, R.C. Wender, "American cancer Society Prostate Cancer Advisory Comitee: American cancer society guideline for the early detection of prostate cancer: update 2010" *CA Cancer J. Clin.*, vol. 60(2), 2010, pp 70-98.

[2] P.Puech, N.Betrouni,"Computer-assisted diagnosis of prostate cancer using DCE-MRI data: design, implementation and preliminary results", *Int J CARS*, vol.4, 2009, pp 1–10.

[3] JS Jones, A. Patel at al. "Saturation technique does not improve cancer detection as an initial prostate biopsy strategy", *J Urol.*, vol. 175(2), 2005, pp 485-488.

[4] S.Candefjord, K. Ramser et al. "Technologies for localization and diagnosis of prostate cancer, review article", *J Med Eng Tech*, vol. 33(8), 2009, pp 585-603.

[5] Warach S, Chien D, et al. "Fast magnetic resonance diffusion-weighted imaging of acute human stroke", *Neurology*, vol.42, 1992; pp 1717–1723.

[6] N.M. DeSouza, S.A Reinsberg, "Magnetic resonace imaging in prostate cancer: the value of apparent diffusion coefficients for identifying malignant nodules", *British Journal of Radiology*, vol. 80, 2007, pp 90-95.

[7] P. Kozlowski, S. D. Chang, S. L. Goldenberg, "Diffusion-weighted MRI in prostate cancer — comparison between single-shot fast spin echo and echo planar imaging sequences", *Magnetic Resonance Imaging*, vol. 26, 2008, pp 72–76.

[8] P. Jezzard, R.S. Balaban, "Correction for geometric distorsion in echo planar images from B0 field variations", *MRM*, vol. 34, 1995, pp 65-73.

[9] Langer DL, van der Kwast TH, et al. "Prostate Cancer Detection With Multi-parametric MRI: Logistic Regression Analysis of Quantitative T2, Diffusion-Weighted Imaging, and Dynamic Contrast-Enhanced MRI", *J Magn Reson Imaging*, vol. 30, 2009, pp 327-334.

[10] D. M. Koh, "Diffusion-weighted MR Imaging, Applications in the body". H. C. Thoeny (Eds.), Springer 2010.